

# Boosting Open-Set Domain Adaptation with Threshold Self-Tuning and Cross-Domain Mixup

Xinghong Liu, Yi Zhou, Tao Zhou, Jie Qin, and Shengcai Liao

**Abstract**—Open-set domain adaptation (OSDA) aims to not only recognize target samples belonging to common classes shared by source and target domains but also perceive unknown class samples. Existing OSDA methods suffer from two obstacles. First, a tedious process of manually tuning a hyperparameter *threshold* is required for most OSDA approaches to separate common and unknown classes. It is difficult to determine a proper threshold when the target domain data is unlabeled. Second, most OSDA methods only rely on confidence values predicted by models to distinguish common/unknown classes. The performance is not satisfied, especially when the majority of the target domain consists of unknown classes. Our experiments demonstrate that combining entropy, consistency, and confidence is a more reliable way of distinguishing common and unknown samples. In this paper, we design a novel threshold self-tuning and cross-domain mixup (TSCM) method to overcome the two drawbacks. TSCM can automatically tune a proper threshold utilizing unlabeled target samples rather than manually setting an empirical hyperparameter. Our method considers multiple criteria instead of only the confidence and uses the threshold generated by itself to separate common and unknown classes in the target domain. Furthermore, we introduce a cross-domain mixup method designed for OSDA scenarios to learn domain-invariant features in a more continuous latent space. Comprehensive experiments illustrate that our method consistently achieves superior performance on different benchmarks compared with various state-of-the-arts.

**Index Terms**—Transfer Learning, Unsupervised Domain Adaptation, Open-Set Domain Adaptation

## I. INTRODUCTION

The most attractive point of deep learning methods is that models [1]–[4] trained on millions of annotated samples can achieve impressive performance on in-distribution new data. However, the performance of trained models usually dramatically drops when they are deployed on the target domain whose domain distribution is significantly different from the source domain. The mismatched domain distribution is called domain shift. It is caused by various perspectives, illumination conditions, and sensors, but can be minimized by transfer learning methods [5], [6] exploiting the information

of labeled target samples. An intuitive way is to label target samples and fine-tune the trained model.

Nevertheless, annotating massive samples on the target domain is time-consuming and costly. To tackle this issue, unsupervised domain adaptation (UDA) approaches [7]–[10] have been proposed to transfer knowledge from an annotated domain to an unlabeled domain. A classic scheme [8], [11], [12] of UDA utilizes domain-hard labels (i.e. marking source samples as 1 and target samples as 0) and then applies a gradient reverse layer to minimize the marginal distribution divergence between source and target domains. In practice, partial samples in the target domain may not belong to any category in the source domain. Thus, more recently, open-set domain adaptation (OSDA) proposed in [13], [14] requires to differentiate those unknown samples whose classes do not appear in the source domain, since forcing to adapt unknown classes with source domains will inevitably lead to negative transfer in OSDA scenarios. We observe that the domain-hard labels will erode the performance of the models. Roughly adopting the domain-hard labels for adaptation will match the whole target domain with the source domain, so the target-private class samples will be wrongly predicted as common classes shared by the source and target domains. Moreover, a tedious process of manually tuning a hyperparameter *threshold* [11], [12], [15]–[18] is usually required to separate common and unknown classes in the target domain. It is difficult to determine a proper threshold when the target domain data is unlabeled.

To address these issues, we propose a module consisting of dual multi-class classifiers (DMC). On the one hand, DMC can guide the model to only align common classes of the target domain instead of the whole target domain with the source domain, which will lead to negative transfer. On the other hand, DMC gradually tunes the threshold based on the confidence toward common classes in different training phases. Therefore, we do not need to manually set a threshold relying on prior experience.

Although DMC alleviates the problems to some extent, we notice that only relying on confidence values generated by DMC is not enough to distinguish common and unknown classes precisely since *confidence* lacks discriminability for the degrees of uncertainty. We need to separate common and unknown classes in the target domain by combining various criteria, such as entropy, consistency, and confidence. *entropy* and *confidence* are complementary to cover both smooth and non-smooth class distributions, and *consistency* can compensate for the confidence for prediction errors [12]. Furthermore, we realize that the limited samples from two

Corresponding author: Yi Zhou

Xinghong Liu and Yi Zhou are with the School of Computer Science and Engineering, Southeast University, Nanjing, China (e-mail: xhml158@gmail.com, yizhou.szcn@gmail.com).

Tao Zhou is with the School of Computer Science and Engineering, Nanjing University of Science and Technology, Nanjing, China (e-mail: taozhou.ai@gmail.com)

Jie Qin is with the College of Computer Science and Technology, Nanjing University of Aeronautics and Astronautics, Nanjing, China (e-mail: qinjie@buaa.edu.cn)

Shengcai Liao is with Inception Institute of Artificial Intelligence (IIAI), Abu Dhabi, U.A.E. (e-mail: shengcai.liao@inceptioniai.org)

domains are insufficient to ensure learning domain-invariant features in the latent space, especially when a large domain gap exists between the source and target domains. Therefore, we design a cross-domain mixup between source and target domains to build a cross-domain bridge for OSDA tasks. Based on the above ideas, we propose a module named multi-criteria discriminator with cross-domain mixup (MDCM).

Overall, we design the DMC and MDCM modules to boost OSDA performance with threshold self-tuning and cross-domain mixup, named as TSCM. TSCM can automatically tune a proper threshold utilizing unlabeled target samples rather than manually setting an empirical threshold. Moreover, our model learns domain-invariant features in a more continuous latent space and precisely separates common/unknown classes relying on multiple criteria. Our contributions are highlighted as follows:

1. To address threshold self-tuning and prevent negative transfer caused by the domain-hard labels, we introduce a dual multi-class classifier (DMC). DMC matches common classes of the two domains, rather than adapting the whole target domain with the source domain. Moreover, DMC can automatically compute an instructive threshold to discriminate common/unknown classes in the target domain. Hence, our method is free from empirically tuning the optimal threshold.

2. We propose a multi-criteria discriminator with cross-domain mixup (MDCM) to distinguish common and unknown classes combining multiple criteria. Our experiments convey that incorporating diverse criteria significantly improves the performance in distinguishing common/unknown samples compared with relying on confidence values. The cross-domain mixup method in MDCM is beneficial for learning domain-invariant features in a smooth latent space despite the large domain gap.

3. Comprehensive experiments have been conducted to compare our method with various state-of-the-arts on three public benchmarks. It illustrates that our model consistently achieves superior performance according to different metrics. Moreover, we carefully study the effectiveness of each proposed component of our method.

## II. RELATED WORK

### A. Unsupervised Domain Adaptation

Unsupervised Domain Adaptation (UDA) performs model training on the target domain without any label information to alleviate performance degradation caused by domain discrepancy. The mathematical essence of UDA is to minimize the joint distribution shift, which can be divided into marginal distribution shift and conditional distribution shift. Ben-David *et al.* [19] theoretically proved that the goal of UDA can be achieved by reducing the inter-domain divergence while maximizing the margin of different categories on the source domain at the same time. Inspired by the generative adversarial network [20], Ganin *et al.* [8] designed an adversarial domain module to measure domain divergence and introduced a gradient reverse layer (GRL) to minimize the marginal distribution shift between source and target domains. GRL can help the model learn domain-invariant features. Wu *et al.*

[21] clarified that the limited number of samples from source and target domains could not guarantee that features in the latent spaces are domain-invariant. They introduced a cross-domain and inter-category mixup method to guide the classifier in learning domain-invariant features in a more continuous latent space. Xu *et al.* [22] proposed a cross-domain mixup method on pixel and feature levels. They applied the mixup method in source and target samples with different ratios to generate various features representing different states between domains. [21], [22] generate a more continuous latent space to guarantee that features are domain-invariant for closed-set domain adaptation after minimizing the marginal distribution shift. Long *et al.* [23] considered that reducing marginal distribution divergence probably cannot precisely align two domains with the multi-modal distribution. They constructed a framework with a conditional discriminator to reduce the conditional distribution difference. Yu *et al.* [10] clarified that the importance of marginal and conditional distributions in real applications is different. They proposed a dynamic adversarial factor to quantitatively evaluate the relative importance of the marginal and conditional distributions. They improved their model performance compared with DANN [8]. These traditional UDA methods are designed for the closed-set domain adaptation (CSDA) task, which cannot be directly applied to open-set domain adaptation problems.

### B. Open-Set Domain Adaptation

Compared with CSDA tasks, the additional challenge for OSDA is that models need to split the target-private classes from the common classes without annotation in target domain. A representative CSDA method labels source and target samples as 1 and 0, respectively, and design a GRL to reduce the marginal distribution divergence of the two domains. Nevertheless, it is not sensible to match the whole target domain with the source domain in OSDA scenarios since it will cause the model to classify the unknown samples into common classes. Saito *et al.* [14] designed a classifier with an additional class *unknown* to discriminate the categories which only exist in the target domain. They proposed an optimization objective with an empirical hyperparameter to train the classifier. Liu *et al.* [24] adopted a coarse-to-fine weighting mechanism to gradually split common and unknown classes in the target domain. Their approach allows weighing the importance of different samples while employing domain adaptation. They also introduced openness, which measures the proportion of unknown classes in all target classes. Shermin *et al.* [25] also had a similar idea like [24]. A supplemental classifier is introduced to assign different weights to each sample. Luo *et al.* [26] proposed a novel method using a graph neural network with episodic training to repress underlying conditional shifts. Subsequently, they adopted adversarial learning to minimize the divergence between source and target domains. Wang *et al.* [27] designed a novel framework called self-ensembling with category-agnostic clusters (SE-CC). They clustered all unlabeled target samples to acquire category-agnostic clusters, which assist in disclosing the underlying feature space structure associated with the target domain. Moreover, they apply

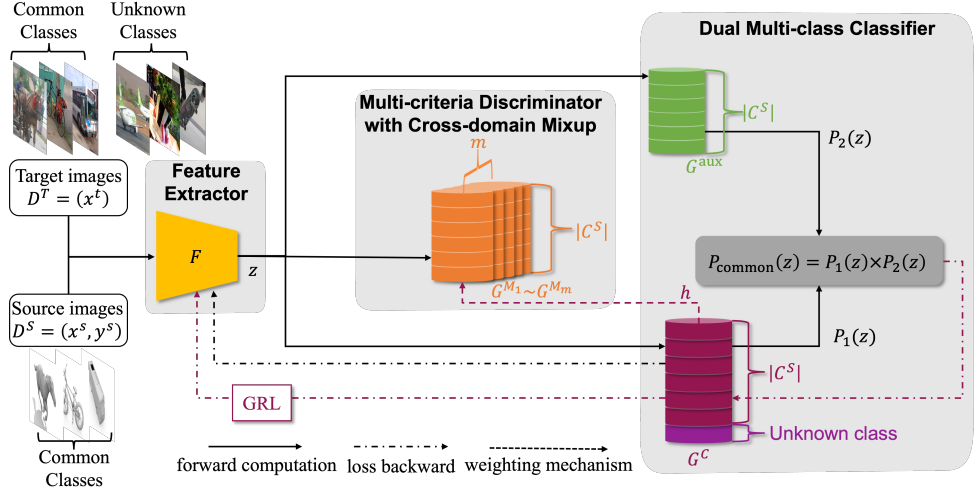


Fig. 1. The architecture of the threshold self-tuning and cross-domain mixup (TSCM) method for open-set domain adaptation.  $F$  is a backbone to extract features. GRL is a gradient reverse layer proposed in [8] to adapt the target domain with the source domain. TSCM contains two modules: multi-criteria discriminator with cross-domain mixup (MDCM) module and dual multi-class classifier (DMC) module. MDCM consists of  $m$  classifiers from  $G^{M_1}$  to  $G^{M_m}$ . DMC consists of two classifiers: an adversarial learning classifier  $G^C$  and an auxiliary classifier  $G^{aux}$ . The outputs  $P_1$  generated by  $G^C$  and  $P_2$  generated by  $G^{aux}$  are utilized to compute the probability  $P_{common}$  that indicates if the sample  $x$  comes from common classes.  $h$  is the instructive threshold computed by  $G^C$  for MDCM to separate common and unknown samples in the target domain.

mutual information to improve the model performance. All the above OSDA methods distinguish common and unknown classes relying on the confidence produced by the model in the testing phase. It is not intensely reliable in some scenarios, especially when the openness of the target domain is large. By contrast, we propose to learn domain-invariant features in a more continuous latent space and combines multiple criteria to precisely separate common/unknown classes.

### III. METHODOLOGY

#### A. Preliminary

In a standard unsupervised domain adaptation (UDA) scenario, we have a source domain  $D^S = \{(x_i^s, y_i^s)\}_{i=1}^{N^S}$  of  $N^S$  labeled samples and a target domain  $D^T = \{(x_i^t)\}_{i=1}^{N^T}$  of  $N^T$  unlabeled samples. The source domain distribution  $p$  is different from the target domain distribution  $q$ . We define a labeled source class set  $C^S$  and an unlabeled target class set  $C^T$ , which are subject to  $C^S \subsetneq C^T$  in open-set domain adaptation (OSDA) scenarios.  $C = C^S \cap C^T$  is the common class set, and  $C = C^S$  in OSDA scenarios.  $C^T \setminus S = C^T \setminus C^S$  denotes the unknown class set. The openness is defined as  $O = 1 - \frac{|C^S|}{|C^T|}$ , where  $|\cdot|$  is the cardinality of a set.

#### B. Overview

Fig.1 illustrates the overall pipeline of the threshold self-tuning and cross-domain mixup (TSCM) model for open-set domain adaptation. TSCM consists of dual multi-class classifier (DMC) module and multi-criteria discriminator with cross-domain mixup (MDCM) module. We utilize the DMC module to adapt the common classes in the target domain with the source domain and generate an instructive threshold  $h$  for MDCM. The MDCM module is used to distinguish common/unknown classes in the target domain. We design

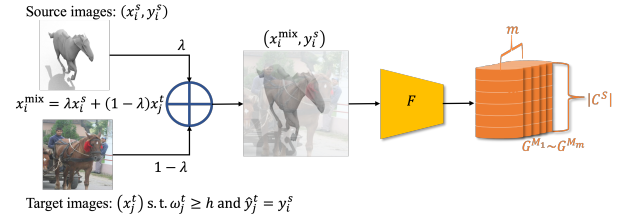


Fig. 2. Cross-domain mixup method in MDCM.  $\hat{y}_j^t$  is the pseudo label of the target sample  $x_j^t$  predicted by  $G^C$ . We will mixup  $x_j^t$  with same class  $x_i^s$  in the pixel level if  $\omega_j^t \geq h$ . The gradients are not back-propagated to the feature extractor  $F$  during MDCM training phases.

a cross-domain mixup method in the MDCM module so the module can learn domain-invariant features in a more continuous latent space. We demonstrate the cross-domain mixup method in the MDCM module in Fig.2.

#### C. Dual Multi-class Classifier

To better improve the alignment performance, we propose the dual multi-class classifier (DMC) module to calculate probabilities to indicate whether each sample belongs to the common classes. The target samples belonging to the common classes and source samples should have high probability values. Therefore, we can adapt the common class in the target domain with the source domain precisely. DMC consists of an adversarial learning classifier  $G^C$  and an auxiliary classifier  $G^{aux}$ .

We define a  $(|C^S|+1)$ -dimension probability vector  $G^C(x)$  predicted by  $G^C$  as follows:

$$G^C(x) = [p_1^{G^C}, p_2^{G^C}, \dots, p_{|C^S|+1}^{G^C}] \quad (1)$$

The probability for the unknown category is indicated by  $(|C^S|+1)$ -th element, and other elements specify the prob-

ability of the corresponding class in  $C^S$ . The samples of common classes in source and target domains tend to have large  $\sum_{c=1}^{|C^S|} p_c^{G^C}$  and small  $p_{|C^S|+1}^{G^C}$ .  $G^C(x)$  is calculated by the following formula:

$$G^C(x) = \frac{\exp(l^{G^C})}{\sum_{c=1}^{|C^S|+1} \exp(l_c^{G^C})}. \quad (2)$$

$l^{G^C}$  is the logit vector projected by  $G^C$  from the feature  $z$ , where  $z = F(x)$ . The loss function of  $G^C$  in the source domain is as follows:

$$\mathcal{E}_{G^C}^S = \mathbb{E}_{x^s \sim p} [\mathcal{L}_{CE}(x^s, y^s)], \quad (3)$$

where  $\mathcal{L}_{CE}$  is a standard cross-entropy loss function.

In addition to  $G^C$ , we design an auxiliary  $|C^S|$ -category classifier  $G^{\text{aux}}$  to compute a probability of a sample belonging to each common class.  $G^{\text{aux}}(x)$  is a  $|C^S|$ -dimension probability vector, which is defined as:

$$G^{\text{aux}}(x) = [p_1^{G^{\text{aux}}}, p_2^{G^{\text{aux}}}, \dots, p_{|C^S|}^{G^{\text{aux}}}] . \quad (4)$$

We calculate  $G^{\text{aux}}(x)$  with a leaky-softmax function [28], which restrains that  $\sum_{c=1}^{|C^S|} p_c^{G^{\text{aux}}}$  (i.e.,  $P_2(x)$  in Fig.1 or Eq.7) is less than 1. If we calculate  $G^{\text{aux}}(x)$  with standard softmax function,  $P_2(x)$  defined in Eq.7 will always be equal to 1. It will cause that we cannot combine  $G^C$  and  $G^{\text{aux}}$  to compute  $P_{\text{common}}(x)$  since  $P_{\text{common}}(x)$  will always equal  $P_1(x)$ .  $G^{\text{aux}}(x)$  is calculated by the following formula:

$$G^{\text{aux}}(x) = \frac{\exp(l^{G^{\text{aux}}})}{|C^S| + \sum_{c=1}^{|C^S|} \exp(l_c^{G^{\text{aux}}})}, \quad (5)$$

where  $l^{G^{\text{aux}}}$  is the logit vector projected by  $G^{\text{aux}}$  from the feature  $z$ . The loss function of  $G^{\text{aux}}$  in the source domain is as follows:

$$\mathcal{E}_{G^{\text{aux}}}^S = \mathbb{E}_{x^s \sim p} [\mathcal{L}_{BCE}(x^s, y'^s)], \quad (6)$$

where  $y'^s$  is the ground-truth label with one-hot format.  $\mathcal{L}_{BCE}$  is a standard binary cross-entropy loss function.

We combine  $G^C$  and  $G^{\text{aux}}$  to identify common class samples.  $P_{\text{common}}$  denotes the probability of a sample  $x$  belonging to common classes, which can be computed by:

$$\begin{aligned} P_{\text{common}}(x) &= P_1(x) \times P_2(x), \\ P_1(x) &= \sum_{c=1}^{|C^S|} p_c^{G^C}, P_2(x) = \sum_{c=1}^{|C^S|} p_c^{G^{\text{aux}}}. \end{aligned} \quad (7)$$

We utilize  $P_{\text{common}}$  to optimize  $G^C$ :

$$\begin{aligned} \mathcal{E}_{G^C, \text{adv}}^D &= \mathbb{E}_{x^t \sim q} \left[ -P_{\text{common}}(x^t) \left( \log p_{|C^S|+1}^{G^C} \right. \right. \\ &\quad \left. \left. + \log \left( 1 - p_{|C^S|+1}^{G^C} \right) \right) \right] \\ &\quad + \mathbb{E}_{x^s \sim p} \left[ - (1 - P_{\text{common}}(x^s)) \left( \log p_{|C^S|+1}^{G^C} \right. \right. \\ &\quad \left. \left. + \log \left( 1 - p_{|C^S|+1}^{G^C} \right) \right) \right]. \end{aligned} \quad (8)$$

For a target sample  $x^t$ , only when  $P_1(x^t)$  and  $P_2(x^t)$  are close to 1, i.e., both  $G^C$  and  $G^{\text{aux}}$  agree  $x^t$  is from common classes,

the model assigns large weight to  $x^t$  and aligns  $x^t$  with the source domain. The model will not align the target samples with small  $P_{\text{common}}(x^t)$  because they only have a small contribution to the loss  $\mathcal{E}_{G^C, \text{adv}}^D$ . For a target sample with a large  $P_{\text{common}}(x^t)$ ,  $G^C$  will decrease the first term and the feature extractor  $F$  will increase the first term because of the GRL's influence. It can cause  $F$  adversarially learns domain-invariant features between target samples from common classes and the source domain. For a source sample  $x^s$ , its  $P_1(x^s)$  and  $P_2(x^s)$  should be close to 1 so its weight  $(1 - P_{\text{common}}(x^s))$  should be close to 0 but not equal to 0. Our experiment demonstrates that the second term (i.e., the expected loss on the source sample  $x^s$ ) can prevent the model from overconfidently classifying unknown class samples as common classes. We argue that the second term can bring a minor perturbation to source sample features so that unknown samples in the target domain cannot be perfectly aligned with the source domain even though the unknown classes are similar to source classes. We use Nuclear-norm Wasserstein discrepancy [29] to train  $G^{\text{aux}}$  to discriminate source and target samples as follows:

$$\mathcal{E}_{G^{\text{aux}}}^D = \mathbb{E}_{x^s \sim p, x^t \sim q} [\|G^{\text{aux}}(x^t)\|_* - \|G^{\text{aux}}(x^s)\|_*], \quad (9)$$

where  $\|\cdot\|$  indicates the Nuclear norm. Notably, as shown in Fig.1, we do not backpropagate the gradient to the feature extractor when we use Eq.9 to optimize the domain discriminability of  $G^{\text{aux}}$ . If we backpropagate the gradient to the feature extractor without GRL, it will catastrophically disrupt its ability to generate domain-invariant features. If we backpropagate the gradient to the feature extractor with GRL, the feature extractor will align the whole target domain with the source domain, which leads to negative transfer.

The optimization objectives of the DMC module can be formulated as:

$$\begin{aligned} \theta_{G^C}^* &= \arg \min_{\theta_{G^C}} \mathcal{E}_{G^C}^S + \mathcal{E}_{G^C, \text{adv}}^D, \\ \theta_F^* &= \arg \min_{\theta_F} \mathcal{E}_{G^C}^S - \mathcal{E}_{G^C, \text{adv}}^D, \\ \theta_{G^{\text{aux}}}^* &= \arg \min_{\theta_{G^{\text{aux}}}} \mathcal{E}_{G^{\text{aux}}}^S + \mathcal{E}_{G^{\text{aux}}}^D. \end{aligned} \quad (10)$$

#### D. Threshold Self-Tuning

Before introducing how to compute the threshold, let us consider three potential situations in the target domain: 1) The potential number of unknown samples is much larger than that of common classes. The threshold needs to be high to prevent classifying numerous unknown samples into common classes. 2) The target domain probably contains many samples of common classes and only a few unknown samples. In this case, the threshold tends to be low. Otherwise, a vast number of common class samples will be labeled with unknown classes. 3) The potential numbers of common class samples and unknown class samples are close. We consider setting the threshold as an intermediate value between the cases of 1) and 2).

The training process is also an important factor for tuning the threshold. Assume  $|C^S| = 2$ , and we have two target samples  $x_1^t, x_2^t$  belonging to class 1 and class 2, both of which are common classes. Since there is a large gap between

source and target domains at the initial stage, the threshold should be close to 1. Hence, only a few target samples, which are extremely similar to source samples, are considered as common classes. As the training progresses, the distribution of source and target domains will be aligned gradually. The threshold will be reduced step by step to classify increasingly more target samples as common classes.

Assume we have two training stages which are indicated as the early and late stage. The target domain is more precisely aligned with the source domain in the late stage. Therefore, we assume to get  $G_{\text{early}}^C(x_1^t) = [0.6, 0.3, 0.1]$ ,  $G_{\text{early}}^C(x_2^t) = [0.3, 0.6, 0.1]$ ,  $G_{\text{late}}^C(x_1^t) = [0.8, 0.1, 0.1]$ , and  $G_{\text{late}}^C(x_2^t) = [0.1, 0.8, 0.1]$ . The threshold in the early stage should be larger than that in the late stage since the model in the early stage has a higher entropy.

According to the above discussion, we propose a formula of the threshold  $h$  produced by  $G^C$  in each epoch:

$$h = 1 - \mathbb{E}_{x_i^t, x_j^t \sim q} \left[ \sum_{c=1}^{|C^S|} (\lambda_1 (G^C(x_i^t) + G^C(x_j^t)) \odot (1 - \lambda_1) (G^C(x_i^t) + G^C(x_j^t))) \right], \quad (11)$$

where  $i, j$  indicates the index number of target samples that are randomly selected.  $\lambda_1 \in [0.5, 1]$  is a hyperparameter used to control the reduction speed. If  $\lambda_1$  closes to 0.5, the threshold drops more rapidly. If  $\lambda_1$  closes to 1, the threshold drops more slowly. Experimental results show that our model is not sensitive to hyperparameter  $\lambda_1$ .  $\odot$  means the element product of two probability vectors. The element product can prevent the threshold from dropping too fast and low and becoming unstable.

Fig.3 shows changes in thresholds on various datasets with different openness. When the openness  $O$  is large, we have a high probability of choosing two unknown samples  $x_i^t, x_j^t$ . The first  $|C^S|$  terms of the output of  $G^C$  will be close to 0 when  $x_i^t, x_j^t$  are unknown samples, so we can get a large threshold  $h$ . On the contrary, we will get a small  $h$ . Furthermore, the first  $|C^S|$  terms of  $G^C(x^t)$  are small in the initial stage of the training phase since  $G^C$  tends to classify most target samples as unknown classes when the target domain is not aligned with the source domain. The threshold  $h$  is large in the early stage to prevent mixing unknown class samples with source samples. We will explain the cross-domain mixup method in the next subsection. As the alignment progresses, the threshold will drop gradually until achieving a proper value.

### E. Multi-criteria Discriminator with Cross-domain Mixup

To better separate unknown class samples of the target domain we propose multi-criteria discriminator with cross-domain mixup (MDCM) module. MDCM can utilize the instructive threshold  $h$  produced by  $G^C$  to classify target samples to common class or unknown class. We introduce a cross-domain mixup method in MDCM. Hence, we can train classifiers in MDCM in a more continuous feature space,

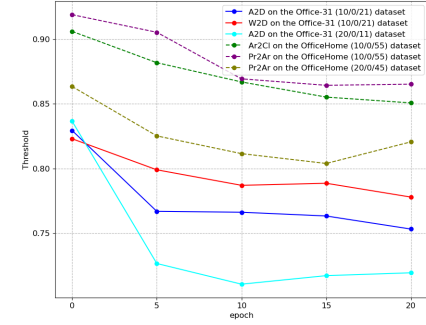


Fig. 3. Changes in thresholds on various datasets with different openness.

especially when the divergence between source and target domain distribution is large.

Specifically, we define a  $|C^S|$ -dimension probability vector  $G^{M_k}(x)$  predicted by each classifier  $G^{M_k}$  in MDCM as follows:

$$G^{M_k}(x) = [p_1^{G^{M_k}}, p_2^{G^{M_k}}, \dots, p_{|C^S|}^{G^{M_k}}]. \quad (12)$$

We calculate  $G^{M_k}(x)$  as the following formula:

$$G^{M_k}(x) = \frac{\exp(l^{G^{M_k}})}{\sum_{c=1}^{|C^S|} \exp(l_c^{G^{M_k}})}. \quad (13)$$

$l^{G^{M_k}}$  is the logit vector projected by  $G^{M_k}$  from the feature  $z$ , where  $z = F(x)$ . As demonstrated in Fig.2, we choose the target samples whose  $\omega^t$  is larger than the instructive threshold  $h$  given by DMC and mixup them in pixel-level manner with the same class samples in the source domain. We propose the cross-domain mixup method for training each classifier  $G^{M_k}$  in MDCM as follows:

$$\begin{aligned} \mathcal{E}_{G^{M_k}} = \mathbb{E}_{(x^s, y^s) \sim p, (x^t) \sim q} [\mathcal{L}_{CE}((1 - \lambda_2)x^s + \lambda_2 x^t, y^s)] \\ \text{s.t. } \omega^t \geq h, \hat{y}^t = y^s, \end{aligned} \quad (14)$$

where  $\lambda_2$  is a hyperparameter controlling the ratio of cross-domain mixup and  $\hat{y}^t$  is the pseudo label of the target sample  $x^t$  predicted by  $G^C$ . Furthermore, we propose a more convenient way to automatically adjust  $\lambda_2$  for MDCM. If we have  $x_1^t, x_2^t$  when  $\omega_1^t > \omega_2^t > h$ , we tend to assign a larger weight  $\lambda_2$  to  $x_1^t$  since the model has higher confidence in confirming  $x_1^t$  comes from the common class. Hence, assigning a higher  $\lambda_2$  to  $x_1^t$  is less likely to have adverse effects, and the model can further learn the characteristics of the target domain. We retrieve  $\lambda_2$  from  $\beta$ -distribution to implement this intuition. The formal definition is as follows:

$$\lambda_2 \sim Beta(\omega^t r, h r) \quad \text{s.t. } \omega^t r > h r > 1, \quad (15)$$

where  $r$  is a coefficient to control the probability density function. Thus, the optimization objective of MDCM is as follows:

$$\theta_{G^{M_k}|_{k=1}^m}^* = \arg \min_{G^{M_k}|_{k=1}^m} \sum_{k=1}^m \mathcal{E}_{G^{M_k}}. \quad (16)$$

Most existing OSDA methods only rely on *confidence*, i.e., the maximum probability mapped by softmax, to determine if a target sample  $x^t$  belongs to a specific common class or the unknown class. Although *confidence* works well when  $|C|$  is large, only considering *confidence* is not a sensible way since it lacks discriminability for the degrees of uncertainty [12]. Our experimental results in Fig.6 illustrate the performance of [14], [25], which only rely on *confidence* to distinguish the common and unknown classes, are poor when  $|C|$  is small. Therefore, it is necessary to separate common/unknown classes based on various criteria. Inspired by [12], we exploit *entropy*, *consistency*, and *confidence* for discriminating common and unknown samples in the target domain.

We utilize probability vectors predicted by  $m$  classifiers in MDCM for a target sample  $x^t$  to calculate *entropy*  $\omega^{\text{ent}}$ , *consistency*  $\omega^{\text{cons}}$ , and *confidence*  $\omega^{\text{conf}}$ . The formal definitions are as follows:

$$\omega^{\text{ent}} = \frac{1}{m} \sum_{k=1}^m \sum_{c=1}^{|C^S|} -p_c^{G^{M_k}} \log(p_c^{G^{M_k}}), \quad (17)$$

$$\omega^{\text{cons}} = \frac{1}{m|C^S|} \sum_{k=1}^m \sum_{c=1}^{|C^S|} \left( p_c^{G^{M_k}} - \frac{1}{m} \sum_{k=1}^m p_c^{G^{M_k}} \right)^2, \quad (18)$$

$$\omega^{\text{conf}} = \frac{1}{m} \sum_{k=1}^m \max(G^{M_k}(x^t)). \quad (19)$$

$\omega^{\text{ent}}$  is large for a target sample of target-private classes and small for common classes.  $\omega^{\text{cons}}$  represents the agreement of multiple classifiers  $G^{M_k}|_{k=1}^m$ , which can compensate for the confidence that usually fails on smooth distribution samples and considers they are uncertain. For smooth distribution,  $\omega^{\text{cons}}$  will be high since classifiers  $G^{M_k}|_{k=1}^m$  in MDCM agree with each other.  $\omega^{\text{conf}}$  is high if MDCM more certainly confirms that a target sample is from common classes. Then we integrate  $\omega^{\text{ent}}$ ,  $\omega^{\text{cons}}$ , and  $\omega^{\text{conf}}$  to compute  $\omega^t$  for a target sample  $x^t$ :

$$\omega^t = \frac{(1 - \omega^{\text{ent}}) + (1 - \omega^{\text{cons}}) + \omega^{\text{conf}}}{3}. \quad (20)$$

Smaller  $\omega^t$  indicates that  $x^t$  is less likely to come from common classes.

The training procedure of TSCM has stated in Algorithm 1. Before training the whole model, we need to pretrain the MDCM module and feature extractor  $F$  only using source samples. The pretraining phase aims to warm up  $F$  and the MDCM module. Therefore, the convergence of TSCM during the training phase can be accelerated, and the noise of pseudo-labels brought by the cross-domain mixup can be alleviated during the training phase. We alternately train DMC and MDCM modules during the training phase. Notably, unlike the pretraining phase, we do not update the parameters of  $F$  when we train the MDCM module during the training phase since we wish to keep the outputs of classifiers in MDCM to be diverse in the test phase.

Finally, Fig.4 shows the architecture of TSCM during testing. In the testing phase, we detach the auxiliary classifier  $G^{\text{aux}}$  from TSCM. TSCM will classify a target sample  $x^t$  as the unknown class if  $\omega^t < h$ . Otherwise, MDCM will further

---

**Algorithm 1** The proposed TSCM

---

**Require:** Labeled source domain  $D^S$ ; Unlabeled target domain  $D^T$ ; Feature extractor  $F$ ; Adversarial learning classifier  $G^C$ ; Auxiliary classifier  $G^{\text{aux}}$ ; Classifiers  $G^{M_1} \sim G^{M_m}$  in the MDCM module.

**Ensure:** Learnt networks  $F$ ,  $G^C$ ,  $G^{\text{aux}}$  and  $G^{M_1} \sim G^{M_m}$ .

- 1: **Pretraining phase:**
- 2: **for**  $i \leftarrow 1$  to  $\text{MaxPreIter}$  **do**
- 3:   **for**  $k \leftarrow 1$  to  $m$  **do**
- 4:     Sample a batch of source samples  $\{x^s, y^s\} \in D^S$
- 5:     Calculate the standard cross-entropy loss of  $G^{M_k}$  by  $\mathcal{E}_{G^{M_k}}^{\text{pre}} = \mathbb{E}_{(x^s, y^s) \sim p} [\mathcal{L}_{CE}(x^s, y^s)]$
- 6:   **end for**
- 7:   Optimize  $F$  and classifiers  $G^{M_1} \sim G^{M_m}$  in the MDCM module by  $\arg \min_{G^{M_k}|_{k=1}^m} \sum_{k=1}^m \mathcal{E}_{G^{M_k}}^{\text{pre}}$
- 8: **end for**
- 9: **Training phase:**
- 10: **for**  $i \leftarrow 1$  to  $\text{MaxEpoches}$  **do**
- 11:   **for**  $j \leftarrow 1$  to  $\text{IterPerEpoch}$  **do**
- 12:     Sample a batch of source data  $\{x^s, y^s\} \in D^S$  and a batch of target data  $\{x^t\} \in D^T$
- 13:     Calculate  $\mathcal{E}_{G^C}^S$  by Eq.3
- 14:     Calculate  $\mathcal{E}_{G^{\text{aux}}}^S$  by Eq.6
- 15:     Calculate  $\mathcal{E}_{G^C, \text{adv}}^D$  by Eq.8
- 16:     Calculate  $\mathcal{E}_{G^{\text{aux}}}^D$  by Eq.9
- 17:     Optimize  $F$ ,  $G^C$  and  $G^{\text{aux}}$  by Eq.10
- 18:   **end for**
- 19:   Calculate the instructive threshold  $h$  by Eq.11
- 20:   **for**  $j \leftarrow 1$  to  $\text{IterPerEpoch}$  **do**
- 21:     **for**  $k \leftarrow 1$  to  $m$  **do**
- 22:       Sample a batch of source data  $\{x^s, y^s\} \in D^S$  and a batch of target data  $\{x^t\} \in D^T$
- 23:       Apply the cross-domain mixup and calculate  $\mathcal{E}_{G^{M_k}}$  by Eq.14
- 24:     **end for**
- 25:     Optimize classifiers  $G^{M_1} \sim G^{M_m}$  in the MDCM module by Eq.16
- 26:   **end for**
- 27: **end for**
- 28: **return**  $F$ ,  $G^C$ ,  $G^{\text{aux}}$  and  $G^{M_1} \sim G^{M_m}$

---

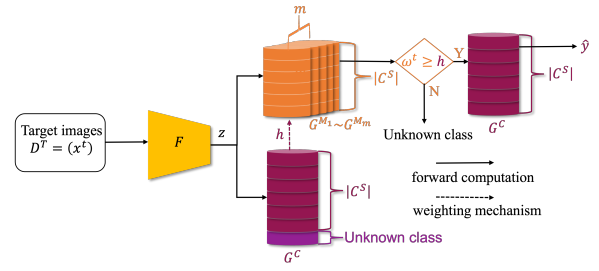


Fig. 4. The architecture of TSCM in the testing phase.

TABLE I  
OS (%) AND H-SCORE (%) ON OFFICE-31 (10/0/21) AND VisDA-2017 (6/0/6) DATASETS

Method	Office-31														VisDA-2017	
	A→D		A→W		D→A		D→W		W→A		W→D		Avg		OS	H-score
	OS	H-score														
DANN [8]	87.83	75.78	77.13	73.16	61.79	72.25	94.48	93.91	65.09	71.07	96.23	94.89	80.43	80.18	51.31	51.41
OSBP [14]	90.82	81.28	86.91	78.62	78.13	73.38	98.36	90.09	75.29	73.69	98.65	92.00	88.03	81.51	62.51	62.78
DAMC [25]	90.61	81.66	86.50	84.21	76.79	79.09	97.38	89.32	75.56	79.93	97.57	84.56	87.40	83.13	40.46	47.60
STA [24]	88.31	39.19	89.56	49.25	78.41	58.38	94.66	58.41	74.08	56.65	93.68	46.77	86.45	51.44	60.52	51.23
PGL [26]	87.91	69.44	83.19	66.45	72.42	59.22	87.84	62.94	75.04	61.06	86.26	67.84	82.11	64.49	<b>72.61</b>	34.57
UADAL [30]	88.14	<b>87.26</b>	84.73	<b>85.59</b>	74.99	77.11	98.33	95.03	70.23	75.86	99.24	95.65	85.94	86.08	59.57	61.26
CMU [12]	87.55	65.55	86.28	63.40	73.43	70.55	96.95	79.83	72.85	69.73	96.51	76.26	86.33	70.89	54.00	51.70
DCC [31]	83.14	83.65	83.99	83.35	<b>80.04</b>	<b>81.81</b>	96.00	92.51	75.49	79.82	98.39	90.27	86.47	84.89	59.33	59.08
OVANet [32]	88.19	81.77	87.62	84.30	66.02	75.51	94.23	95.62	68.56	77.60	98.94	93.83	83.93	84.77	46.13	57.53
TSCM	<b>91.32</b>	84.65	<b>90.20</b>	85.05	77.43	81.29	<b>99.71</b>	<b>98.37</b>	<b>77.15</b>	<b>81.58</b>	<b>99.66</b>	<b>98.07</b>	<b>89.23</b>	<b>88.17</b>	63.59	<b>63.23</b>

TABLE II  
OS (%) AND H-SCORE (%) ON THE OFFICE-HOME (10/0/55) DATASET

Method	Office-Home														Avg			
	Pr→Ar		Pr→Cl		Pr→Rw		Rw→Ar		Rw→Cl		Rw→Pr		OS	H-score				
OS	H-score	OS	H-score	OS	H-score	OS	H-score	OS	H-score	OS	H-score	OS	H-score	OS	H-score			
DANN [8]	52.72	61.94	66.23	71.86	71.39	74.79	49.79	53.48	68.47	70.46	61.06	66.50	52.05	57.55	45.83	53.51		
OSBP [14]	58.66	59.41	71.50	66.09	79.18	70.58	71.81	66.78	71.79	69.20	72.34	66.65	<b>66.49</b>	53.10	54.87	78.50	69.63	
DAMC [25]	54.04	59.40	66.26	70.10	76.48	74.20	67.65	<b>67.14</b>	74.67	66.50	66.86	67.34	62.32	65.96	49.66	56.94	78.62	
STA [24]	61.47	43.50	73.64	47.96	80.30	43.94	67.19	37.62	79.90	36.68	74.94	34.78	67.61	53.41	<b>57.94</b>	39.51	<b>63.22</b>	
PGL [26]	<b>64.05</b>	53.29	75.39	58.04	<b>83.23</b>	60.77	<b>68.64</b>	55.29	<b>82.50</b>	59.95	<b>81.69</b>	59.89	<b>71.89</b>	20.41	46.93	42.29	77.06	51.47
UADAL [30]	63.24	61.08	73.40	70.84	80.96	76.27	65.26	62.18	82.48	71.38	73.02	66.93	59.19	64.48	55.46	<b>60.01</b>	73.99	
CMU [12]	45.63	55.94	59.02	68.50	67.80	74.14	46.28	55.84	57.69	65.95	58.38	66.27	42.06	52.50	39.88	49.83	60.75	
DCC [31]	54.45	57.03	<b>76.30</b>	73.81	81.70	<b>79.85</b>	56.18	35.00	68.87	<b>74.62</b>	67.52	68.93	47.18	55.74	45.87	52.60	74.01	
OVANet [32]	55.03	63.20	70.27	73.03	78.64	75.11	58.05	64.15	78.91	68.63	71.40	66.74	52.12	61.02	46.82	55.66	70.97	
TSCM	54.48	<b>63.35</b>	72.75	<b>74.26</b>	78.88	78.26	62.67	66.16	74.73	72.22	68.41	<b>70.14</b>	61.93	66.30	49.19	57.30	68.27	

deliver  $x^t$  to  $G^C$ , and then  $G^C$  classifies  $x^t$  into a specific common class.

#### IV. EXPERIMENTS

##### A. Setup

We choose three benchmarks to evaluate our model and compare our method with state-of-the-art approaches for open-set domain adaptation on object recognition. We use the label file provided by [33], [34] as the label list.

**Office-31** [35] is a benchmark for domain adaptation, which contains 31 object classes in 3 domains: Amazon (**A**), DSLR (**D**) and Webcam (**W**). We choose the first 10 categories in label order as the common classes and the samples from the remaining 21 classes as private samples of the target domain. The label order in the file is the same as in alphabetical order.

**Office-Home** [36] is a challenging dataset for computer vision domain adaptation, which contains 65 categories in 4 domains: Art (**Ar**), Clipart (**Cl**), Product (**Pr**) and Real-World (**Rw**). We follow [25] to construct the first 10 classes as the common classes shared by the source and target domains and other categories as the unknown class. We also use label order to sort the classes. The label order in the label file is different from the alphabetical order. Specifically, the first 10 classes are Drill, Exit Sign, Bottle, Glasses, Computer, File Cabinet, Shelf, Toys, Sink, and Laptop. The advantage of following label order is that we can evaluate model performances on the categories even though their first letter is at the end of the Office-Home dataset in alphabetical order.

**VisDA-2017** [37] focus on adapting synthetic images to real images across 12 classes in 2 domains: synthetic and real. We follow label order to divide 6 categories into common classes for source and target domains and 6 classes to be the private class of the target domain. The label order in the file is the same as in alphabetical order. This setting validates the efficiency of our model on large-scale domain adaptation tasks.

**Evaluation Metric.** We employ two metrics to evaluate the performance of different methods: **OS** and **H-score** [12], [38]. OS can estimate the average accuracy for  $|C| + 1$  classes consisting of  $|C|$  common classes and the unknown as one class. H-score is the harmonic mean of the accuracy of  $OS^*$  on common classes  $C$  and the accuracy of  $Unk$  on the unknown class. The formalization of the H-score is as follows:

$$H_{score} = 2 \times \frac{OS^* \times Unk}{OS^* + Unk} \quad (21)$$

**Compared State-of-the-Arts.** We have compared TSCM with: 1) Modified closed-set domain adaptation method: DANN proposed in [8], and it was modified by [33], [34] so that it can work on OSDA scenarios. 2) Open-set domain adaptation methods: OSBP [14], DAMC [25], STA [24], PGL [26] and UADAL [30]. 3) Universal domain adaptation (UniDA) methods: CMU [12], DCC [31] and OVANet [32]. UniDA methods assume that both source and target domains have private classes, so UniDA methods natively support OSDA tasks.

**Implementation Details.** We adopt ResNet-50 [1] pre-trained on ImageNet [39] as the backbone to extract features for fair comparisons. We use Nesterov momentum SGD with the momentum of 0.9 and weight decay of  $5 \times 10^{-4}$  to optimize our model. We follow [12] decaying the learning rate with the factor of  $(1 + \gamma \times i)^{-\beta}$ , where  $i$  denotes the current iteration, and we set  $\gamma = 0.001$  and  $\beta = 0.75$ .  $\lambda_1 = 0.5$  in Eq.11,  $\lambda_2 = 0.5$  in Eq.14, and  $r = 30$  in Eq.15. We set  $m = 5$  classifiers in the MDCM module. We follow [12] to use different data augmentations for MDCM to enable more diverse classifiers. All experiment is done on  $1 \times 3090$  GPU. The code is available on GitHub.<sup>1</sup>

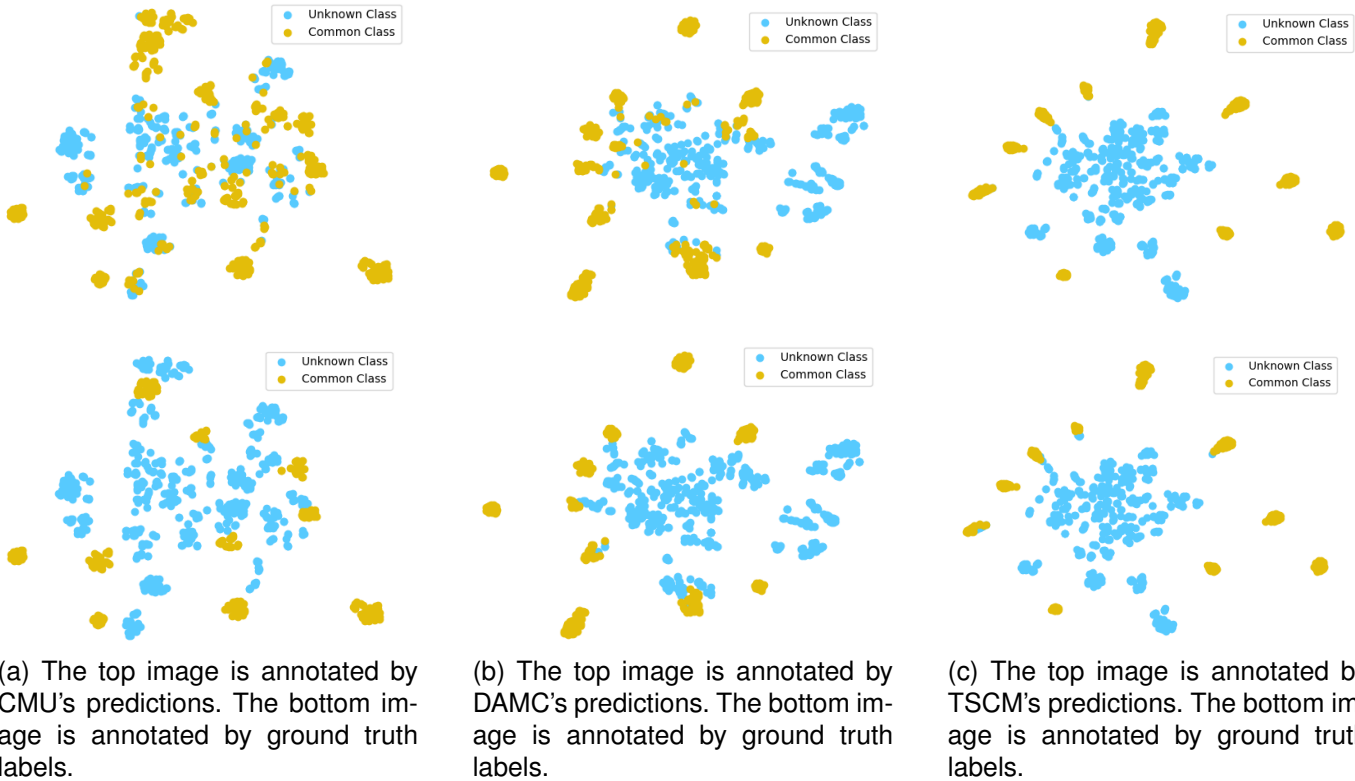


Fig. 5. An example of feature visualization with t-SNE [40] for the **D**→**W** task on the Office-31 dataset. We compare our method with CMU [12] and DAMC [25] on separating common/unknown target samples. We choose the epoch with the best H-score and visualize target sample predictions. Plots in yellow are common samples, and in blue are unknown samples.

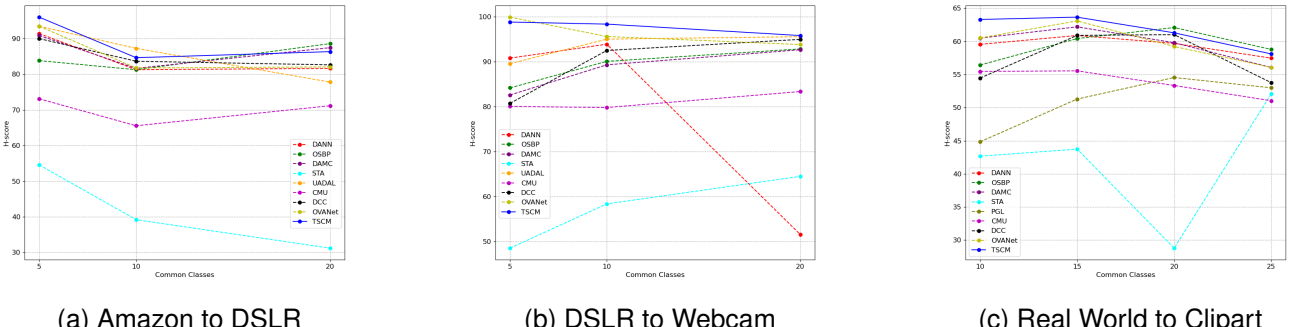


Fig. 6. H-score in varying sizes of  $|C|$ . We change  $|C|$  on Office-31 and Office-Home.

### B. Comparison with State-of-the-Arts

The classification results of Office-31 and VisDA-2017 are shown in Table I, and the results of Office-Home are shown in Table II. We compute the H-score on all datasets and OS for Office-31, VisDA-2017, and Office-Home datasets. We choose ResNet-50 [1] as the feature extractor for fair comparisons.

Our proposed method outperforms all the previous methods in terms of OS and H-score on the Office-31 dataset. We can infer that our method works well and exceeds other methods when there is a small domain gap between source and target domains. Moreover, our method outperforms the compared methods on the Office-Home dataset on H-score. The results

show that when we deal with OSDA tasks, which are more challenging in large domain gaps and disjoint label space between the source and target domains, TSCM exceeds the performance of existing OSDA methods by large margins on most tasks of distinguishing common and unknown samples. The results show TSCM can adapt the common classes in the target domain to the source domain even though there is a significant gap between source and target domains. We notice that the performance of our model on OS scores still has room for improvement, which will be the research direction of our future work.

Our method consistently performs best and significantly improves OS and H-score on the VisDA-2017 dataset com-

<sup>1</sup><https://github.com/XHomL/TSCM.git>

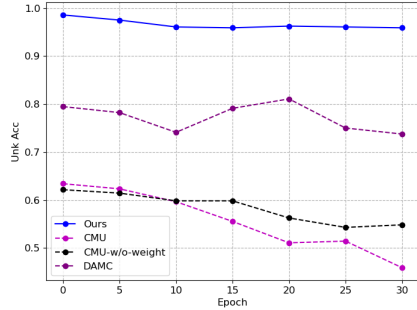


Fig. 7. The unknown class accuracy of different methods for the  $\mathbf{D} \rightarrow \mathbf{W}$  task on the Office-31 dataset. CMU [12] and DAMC [25] are compared. CMU-w/o-weight denotes removing sample weights  $\omega^s$  and  $\omega^t$  in the domain adversarial discriminator of CMU.

pared to most methods except PGL. PGL has a high OS but a low H-score. It implies that PGL tends to classify a vast number of target-private samples into common classes. In fact, We do not expect this behavior to happen on OSDA tasks. Overall, the results on the VisDA-2017 dataset indicate that TSCM can learn semantic information from synthetic images and adapt the information to real images shot in diverse scenarios. The results on the VisDA-2017 dataset are more convincing than Office-31 or Office-Home datasets since the dataset contains abundant images. Therefore, random factors on samples only slightly affect the models' performance on OS and H-score. Furthermore, the VisDA-2017 dataset can evaluate the robustness of methods for classifying images with complex scenes.

### C. Analysis

**Distinguishing common and unknown data.** In order to reduce the marginal distribution divergence between source and target domains, Ganin *et al.* [8] construct an adversarial network with domain-hard labels to fool the domain discriminator and then align the whole target domain with the source domain. Nevertheless, those intuitive ideas designed for close-set domain adaptation will induce the models to match the target-private classes with the common classes in OSDA scenarios. Hence, mass unknown class samples will be classified as common classes. Some researchers [11], [12] proposed to compute weights  $\omega^s$  for each source sample and  $\omega^t$  for each target sample, then deliver to the explicit domain discriminator to distinguish common and unknown classes more accurately. Fig.5 shows an example of the feature visualization with t-SNE [40] for the  $\mathbf{D} \rightarrow \mathbf{W}$  task on the Office-31 dataset. Fig.7 is the unknown class accuracy of TSCM, CMU [12] and DAMC [25] in the domain adaptation task  $\mathbf{D} \rightarrow \mathbf{W}$  on the Office-31 dataset. The performance of CMU [12] in separating common and unknown classes is still poor, as shown in Fig.5a. Furthermore, CMU is less stable than the model without assigning weights  $\omega^s$  and  $\omega^t$  as Fig.7 shows. As shown in Fig. 5a, 5c and 7, our model performs better in distinguishing common/unknown classes than models with domain-hard labels like CMU [12] that induce aligning the whole target domain with the source

domain. The domain-hard labels lead to matching the whole target domain with the source domain, and it causes the model to label numerous target-private samples to common classes as shown in Fig.5a. The contributions of allocating weights  $\omega^s$  and  $\omega^t$  are just a drop in the bucket, and the model will become less stable. Compared with DAMC [25], which only relies on the confidence to distinguish common and unknown classes, we construct the MDCM module to exploit various information. Comparing Fig.5b, 5c and 7, we can conclude that our method performs better and is more stable than DAMC in separating common/unknown classes. The results indicate that our method can precisely identify common class samples from source and target domains and matches them, so it can avoid classifying target-private samples as common classes.

### Varying Sizes of the Number of Common Classes $|C|$ .

The performances of the H-score across various numbers of common classes  $|C|$  on Office-31 and Office-Home datasets are visualized in Fig.6. When there are more unknown classes, correctly separating target classes relying only on confidence values is hard. TSCM overcomes the drawback of OSBP [14] and DAMC [25], and it works well when the openness  $O$  is large. Furthermore, we notice some models, e.g. UADAL, OSBP, DAMC, STA, do not perform well on  $\mathbf{D} \rightarrow \mathbf{W}$  OSDA tasks if  $|C|=5$ . It implies that when two domains are similar and  $O$  is large, relying on the confidence is not a reliable way to separate common/unknown samples. The models will recognize unknown samples as common class samples. The performances of TSCM are also better for most methods when we increase  $|C|$ . As we mentioned above, the models relying on the confidence can achieve good performances on OSDA tasks if we have a small openness  $O$ . TSCM can provide comparable performances when we reduce  $O$ , which means TSCM is more general on various  $O$  on different OSDA tasks. For most tasks, CMU [12] and DANN [8] work poorly on different  $O$ . It indicates that domain-hard labels will negatively impact open-set domain adaptation.

**Ablation Studies.** We evaluate the effectiveness of the proposed components in TSCM on Office-31, Office-Home and VisDA-2017 datasets separately. 1)  $G^C$ -w/o-2nd-term means that we remove the second term in Eq.8. 2) TSCM-w/o- $G^{\text{aux}}$  represents that we remove  $G^{\text{aux}}$  in the DMC module and we rely only  $G^C$  to compute the weight in Eq.8 to align target and source domains. In this case,  $P_{\text{common}}(x) = P_1(x)$  in Eq.8 instead of  $P_{\text{common}}(x) = P_1(x) \times P_2(x)$ . 3) TSCM-w/o-MDCM denotes that we remove the MDCM module and use the output of  $G^C$  to predict the target samples' classes. If  $\forall p_c^{G^C} \geq h, c \in [1, |C^S|]$ , we classify the target sample as the common class  $c$ . Otherwise, we predict the target sample as unknown. 4) TSCM-w/o-MDCM-h is similar to the 3) case, but we use the maximum confidence  $\max(p_c^{G^C}), c \in [1, |C^S| + 1]$  rather than compare the confidence with the threshold to predict the target sample's class  $c$ . 5) TSCM-w/o-mixup denotes that we do not use the cross-domain mixup in the MDCM module. 6) TSCM-w- $\beta$  represents that we let the model automatically retrieve  $\lambda_2$  in Eq.13 from Eq.15.

The results in Tables III and IV show that the second term in Eq.8 is beneficial for the model to separate common/unknown

TABLE III  
OS (%) AND H-SCORE (%) OF ABLATION STUDIES ON OFFICE-31 (10/0/21) AND VisDA-2017 (6/0/6) DATASET

Method	Office-31												VisDA-2017	
	A→D		A→W		D→A		D→W		W→A		W→D		Avg	
	OS	H-score	OS	H-score	OS	H-score	OS	H-score	OS	H-score	OS	H-score	OS	H-score
$G^C$ -w/o-2nd-term	92.72	82.60	92.70	84.54	76.32	78.44	99.22	97.09	77.12	80.27	99.18	95.28	89.54	86.37
TSCM-w/o- $G^{\text{aux}}$	90.17	84.43	92.58	86.37	72.60	78.75	99.63	97.90	75.21	81.67	99.71	98.38	88.32	87.92
TSCM-w/o-MDCM	92.25	86.96	85.62	85.42	64.78	74.23	91.75	94.67	65.97	75.76	99.26	98.94	83.27	86.00
TSCM-w/o-MDCM- $h$	82.56	81.48	89.56	80.60	75.39	78.07	98.03	94.39	73.83	78.14	99.10	94.80	86.41	84.58
TSCM-w/o-mixup	90.88	85.38	88.60	85.46	74.48	80.93	99.69	98.27	73.22	80.44	99.66	98.07	87.76	88.09
TSCM-w- $\beta$	91.96	85.10	90.82	84.19	76.13	81.44	99.68	98.18	75.32	81.14	99.60	97.77	88.92	87.97
TSCM	91.32	84.65	90.20	85.05	77.43	81.29	99.71	98.37	77.15	81.58	99.66	98.07	89.23	88.17

TABLE IV  
OS (%) AND H-SCORE (%) OF ABLATION STUDIES ON THE OFFICE-HOME (10/0/55) DATASET

Method	Office-Home												Avg	
	Ar	OS	H-score	Ar	OS	H-score	Cl	OS	H-score	Cl	OS	H-score	OS	H-score
$G^C$ -w/o-2nd-term	55.98	61.95	73.29	71.88	80.15	76.31	66.84	72.33	70.86	71.01	68.52	59.53	65.98	48.91
TSCM-w/o- $G^{\text{aux}}$	54.71	62.30	72.44	73.54	79.64	77.40	64.47	66.89	73.92	72.26	69.83	70.09	60.94	65.90
TSCM-w/o-MDCM	45.28	55.85	62.87	71.51	68.42	75.46	48.91	59.13	69.23	73.53	61.36	68.33	43.19	59.93
TSCM-w/o-MDCM- $h$	56.10	59.38	73.04	70.81	79.92	75.44	69.58	64.52	78.73	64.32	73.96	64.04	64.49	54.63
TSCM-w/o-mixup	51.33	60.97	69.21	75.02	77.46	78.69	61.34	66.86	71.09	71.88	70.46	55.61	64.10	45.50
TSCM-w- $\beta$	55.06	63.39	71.14	74.01	79.58	78.15	63.92	66.69	72.87	72.08	69.25	59.93	65.07	47.49
TSCM	54.48	63.35	72.75	74.26	78.88	78.26	62.67	66.16	74.73	72.22	68.41	70.14	61.93	46.30

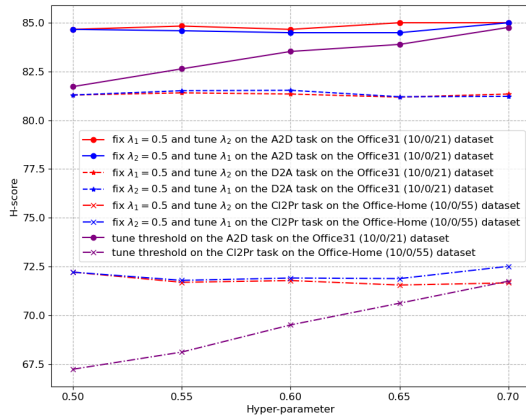


Fig. 8. Sensitivity of hyperparameters  $\lambda_1$  and  $\lambda_2$ .  $\lambda_1$  is for controlling the rate of descent of threshold  $h$  in Eq.11, and  $\lambda_2$  is for the mixup ratio in Eq.14.

samples. It prevents the model from incorrectly classifying unknown samples as common classes. The auxiliary classifier  $G^{\text{aux}}$  assists the model in computing a more suitable weight  $P_{\text{common}}$  to align the two domains more precisely. TSCM-w/o-MDCM and TSCM-w/o-MDCM- $h$  demonstrate that combining *entropy*, *consistency*, and *confidence* is a more reliable way to distinguish common/unknown classes compared with only depending on the confidence. According to the results of TSCM-w/o-mixup, we can infer that the cross-domain mixup method can help TSCM learn domain-invariant features in a more continuous feature space when there is a large gap between source and target domains. TSCM-w- $\beta$  achieves comparable performance with TSCM, which means TSCM can extract suitable mixup parameter  $\lambda_2$  from  $\beta$ -distribution by itself.

**Robustness of Hyperparameters.** We tune the hyperparameters  $\lambda_1$  in Eq.11 and  $\lambda_2$  in Eq.14 on **A→D** and **D→A** tasks of the Office-31 dataset and the **Cl→Pr** task of the Office-Home dataset. The results in Fig.8 show our

TABLE V  
OS (%) AND H-SCORE (%) WITH VARIOUS  $m$  AND  $\beta$  ON OFFICE-31 (10/0/21), OFFICE-HOME (10/0/55) AND VisDA-2017 (6/0/6) DATASETS

Hyperparameters	Office-31		Office-Home		Visda-2017	
	OS	H-score	OS	H-score	OS	H-score
$m=3$	88.55	87.99	65.49	69.47	63.21	63.38
$m=4$	88.54	87.72	66.37	69.23	63.15	63.72
$m=5$	89.23	88.17	65.97	69.55	63.59	63.23
$\beta=10$	89.10	88.03	65.97	69.23	61.22	63.38
$\beta=20$	89.05	87.89	65.97	69.23	61.25	63.33
$\beta=30$	88.92	87.97	65.34	69.32	63.55	62.13

method is not sensitive to changing hyperparameters  $\lambda_1$  and  $\lambda_2$ . Compared with tuning the threshold, which significantly influences the model's performance, the model has stable performance with various  $\lambda_1$  and  $\lambda_2$ . Hence, our method is free from empirically tuning the optimal threshold. We explore the various numbers  $m$  of classifiers in the MDCM module and  $\beta$  in Eq.15. The results in Table V convey that TSCM maintains steady performance with different  $m$  and  $\beta$ .

## V. CONCLUSION

In this paper, we propose a novel threshold self-tuning and cross-domain mixup (TSCM) method for open-set domain adaptation. TSCM consists of two modules: dual multi-class classifier (DMC) and multi-criteria discriminator with cross-domain mixup (MDCM). DMC can align common classes in the target domain instead of the whole target domain with the source domain and utilize unlabeled target samples to compute a suitable threshold for MDCM. MDCM combines entropy, consistency, confidence, and the instructive threshold computed by DMC to separate common/unknown samples in the target domain. Moreover, the cross-domain mixup method can guide MDCM in learning domain-invariant features in a more continuous latent space. The experimental results on three OSDA benchmarks show that the TSCM model is superior to state-of-the-arts, especially when the openness  $O$  is large. In addition, TSCM is not sensitive to hyperparameters and has stable performance. We expect to extend our work to universal domain adaptation tasks in future works.

## REFERENCES

- [1] K. He, X. Zhang, S. Ren, and J. Sun, “Deep residual learning for image recognition,” in *CVPR 2016*, pp. 770–778.
- [2] K. Simonyan and A. Zisserman, “Very deep convolutional networks for large-scale image recognition,” in *ICLR 2015*.
- [3] S. Ren, K. He, R. B. Girshick, and J. Sun, “Faster R-CNN: towards real-time object detection with region proposal networks,” in *NeurIPS 2015*, pp. 91–99.
- [4] K. He, G. Gkioxari, P. Dollár, and R. B. Girshick, “Mask R-CNN,” in *ICCV 2017*, pp. 2980–2988.
- [5] J. Quiñonero-Candela, M. Sugiyama, A. Schwaighofer, N. D. Lawrence, A. Storkey, D. Corfield, M. Hein, L. K. Hansen, S. Ben-David, and T. Kanamori, *Dataset Shift in Machine Learning*. Cambridge: MIT Press, 2008.
- [6] S. J. Pan and Q. Yang, “A survey on transfer learning,” *IEEE Trans. Knowl. Data Eng.*, vol. 22, no. 10, pp. 1345–1359, 2010.
- [7] M. Long, Y. Cao, J. Wang, and M. I. Jordan, “Learning transferable features with deep adaptation networks,” in *ICML 2015*, pp. 97–105.
- [8] Y. Ganin, E. Ustinova, H. Ajakan, P. Germain, H. Larochelle, F. Laviolette, M. Marchand, and V. S. Lempitsky, “Domain-adversarial training of neural networks,” *J. Mach. Learn. Res.*, vol. 17, pp. 59:1–59:35, 2016.
- [9] J. Wang, Y. Chen, W. Feng, H. Yu, M. Huang, and Q. Yang, “Transfer learning with dynamic distribution adaptation,” *ACM Trans. Intell. Syst. Technol.*, vol. 11, no. 1, pp. 6:1–6:25, 2020.
- [10] C. Yu, J. Wang, Y. Chen, and M. Huang, “Transfer learning with dynamic adversarial adaptation network,” in *ICDM 2019*, pp. 778–786.
- [11] K. You, M. Long, Z. Cao, J. Wang, and M. I. Jordan, “Universal domain adaptation,” in *CVPR 2019*, pp. 2720–2729.
- [12] B. Fu, Z. Cao, M. Long, and J. Wang, “Learning to detect open classes for universal domain adaptation,” in *ECCV 2020*, pp. 567–583.
- [13] P. P. Bustos and J. Gall, “Open set domain adaptation,” in *ICCV 2017*, pp. 754–763.
- [14] K. Saito, S. Yamamoto, Y. Ushiku, and T. Harada, “Open set domain adaptation by backpropagation,” in *ECCV 2018*, pp. 156–171.
- [15] L. P. Jain, W. J. Scheirer, and T. E. Boult, “Multi-class open set recognition using probability of inclusion,” in *ECCV 2014*, pp. 393–409.
- [16] A. Bendale and T. E. Boult, “Towards open set deep networks,” in *CVPR 2016*, pp. 1563–1572.
- [17] P. R. M. Júnior, R. M. de Souza, R. de Oliveira Werneck, B. V. Stein, D. V. Pazinato, W. R. de Almeida, O. A. B. Penatti, R. da Silva Torres, and A. Rocha, “Nearest neighbors distance ratio open-set classifier,” *Mach. Learn.*, vol. 106, no. 3, pp. 359–386, 2017.
- [18] Z. Ge, S. Demyanov, and R. Garnavi, “Generative openmax for multi-class open set classification,” in *BMVC 2017*.
- [19] S. Ben-David, J. Blitzer, K. Crammer, and F. Pereira, “Analysis of representations for domain adaptation,” in *NeurIPS 2007*, pp. 137–144.
- [20] I. J. Goodfellow, J. Pouget-Abadie, M. Mirza, B. Xu, D. Warde-Farley, S. Ozair, A. C. Courville, and Y. Bengio, “Generative adversarial nets,” in *NeurIPS 2014*, pp. 2672–2680.
- [21] Y. Wu, D. Inkpen, and A. El-Roby, “Dual mixup regularized learning for adversarial domain adaptation,” in *ECCV 2020*, pp. 540–555.
- [22] M. Xu, J. Zhang, B. Ni, T. Li, C. Wang, Q. Tian, and W. Zhang, “Adversarial domain adaptation with domain mixup,” in *AAAI 2020*, pp. 6502–6509.
- [23] M. Long, Z. Cao, J. Wang, and M. I. Jordan, “Domain adaptation with randomized multilinear adversarial networks,” *CoRR*, vol. abs/1705.10667, 2017.
- [24] H. Liu, Z. Cao, M. Long, J. Wang, and Q. Yang, “Separate to adapt: Open set domain adaptation via progressive separation,” in *CVPR 2019*, pp. 2927–2936.
- [25] T. Shermin, G. Lu, S. W. Teng, M. M. Murshed, and F. Sohel, “Adversarial network with multiple classifiers for open set domain adaptation,” *IEEE Trans. Multim.*, vol. 23, pp. 2732–2744, 2021.
- [26] Y. Luo, Z. Wang, Z. Huang, and M. Baktashmotlagh, “Progressive graph learning for open-set domain adaptation,” in *ICML 2020*, pp. 6468–6478.
- [27] Y. Pan, T. Yao, Y. Li, C. Ngo, and T. Mei, “Exploring category-agnostic clusters for open-set domain adaptation,” in *CVPR 2020*, pp. 13864–13872.
- [28] Z. Cao, K. You, M. Long, J. Wang, and Q. Yang, “Learning to transfer examples for partial domain adaptation,” in *CVPR 2019*, pp. 2985–2994.
- [29] L. Chen, H. Chen, Z. Wei, X. Jin, X. Tan, Y. Jin, and E. Chen, “Reusing the task-specific classifier as a discriminator: Discriminator-free adversarial domain adaptation,” in *CVPR 2020*, June 2022, pp. 7181–7190.
- [30] J. Jang, B. Na, D. Shin, M. Ji, K. Song, and I. Moon, “Unknown-aware domain adversarial learning for open-set domain adaptation,” *CoRR*, vol. abs/2206.07551, 2022.
- [31] G. Li, G. Kang, Y. Zhu, Y. Wei, and Y. Yang, “Domain consensus clustering for universal domain adaptation,” in *CVPR 2021*, pp. 9757–9766.
- [32] K. Saito and K. Saenko, “Ovanet: One-vs-all network for universal domain adaptation,” in *ICCV 2021*, pp. 8980–8989.
- [33] J. Jiang, Y. Shu, J. Wang, and M. Long, “Transferability in deep learning: A survey,” 2022.
- [34] J. Jiang, B. Chen, B. Fu, and M. Long, “Transfer-learning-library,” <https://github.com/thuml/Transfer-Learning-Library>, 2020.
- [35] K. Saenko, B. Kulic, M. Fritz, and T. Darrell, “Adapting visual category models to new domains,” in *ECCV 2010*, pp. 213–226.
- [36] H. Venkateswara, J. Eusebio, S. Chakraborty, and S. Panchanathan, “Deep hashing network for unsupervised domain adaptation,” in *CVPR 2017*, pp. 5385–5394.
- [37] X. Peng, B. Usman, N. Kaushik, J. Hoffman, D. Wang, and K. Saenko, “Visda: The visual domain adaptation challenge,” *CoRR*, vol. abs/1710.06924, 2017.
- [38] S. Bucci, M. R. Loghmani, and T. Tommasi, “On the effectiveness of image rotation for open set domain adaptation,” in *ECCV 2020*, pp. 422–438.
- [39] J. Deng, W. Dong, R. Socher, L. Li, K. Li, and L. Fei-Fei, “Imagenet: A large-scale hierarchical image database,” in *CVPR 2009*, pp. 248–255.
- [40] L. van der Maaten and G. Hinton, “Visualizing data using t-sne,” *Journal of Machine Learning Research*, vol. 9, no. 86, pp. 2579–2605, 2008.